A New IDMA System Based on CSK Modulation for Multiuser Underwater Acoustic Communications

Lianyou Jing, Chengbing He, *Member, IEEE*, Han Wang, Qunfei Zhang, *Member, IEEE*, and Hongxi Yin

***Abstract*—This work proposes a novel interleave-division multiple access (IDMA) system based on cyclic shift keying (CSK) modulation, named CSK-IDMA, for multiuser underwater acoustic (UWA) communications. The CSK modulation uses a circular cyclic shift of the spreading sequence to represent the information, which can be viewed as a special M-ary spread spectrum modulation. Compared with conventional direct-sequence spread spectrum (DSSS) technique, CSK overcomes the spreading gain versus data rate limitations. The proposed scheme adopts the IDMA technique to reduce the cochannel interference. At the receiver, we employ passive time reversal (PTR) technique to compress the channels and improve the signal-to-interference-noise ratio (SINR) at first. In order to perfectly incorporate with the IDMA receive structure, we propose a soft CSK demodulation which can iteratively exchange extrinsic information with a soft channel decoder to form a turbo equalization. Simulation results show the proposed CSK-IDMA scheme can offer significantly improved performance. The data processing results from a lake experiment show that the proposed scheme can support 8 users and 10 users with zero error bits for 2.3 km transmission and 2.7 km transmission, respectively. The corresponding bit error rate (BER) for 16 users are 8.4×10^{-4} and 9.7×10^{-4}, respectively. The data rate is 62.5 bit/s per user within 4 kHz bandwidth and spreading sequences of 256 chips. To the best of our knowledge, this is the first work which can support more than 8 users for multiuser UWA communications with a high bandwidth efficiency.**

***Index Terms*—Interleave-division multiple access (IDMA), cyclic shift keying (CSK), soft demodulation, multiuser underwater acoustic communication.**

I. Introduction

With the rapid development of ocean exploitation, more and more autonomous underwater vehicles (AUVs) or unmanned underwater vehicles (UUVs) are equipped to handle long-range missions and carry out various tasks, such as oil exploration, pollution monitoring and scientific data collections, etc. [1]. The vehicles need to communicate with each other to cooperate and the base station to receive the control instruction when the AUVs or UUVs are working. So far, underwater acoustic (UWA) communication is the only technology to realize medium and long-range underwater communication. UWA communications, especially multiuser UWA communications, are a vital part of the underwater vehicles system. However, the characteristics of UWA channels have always limited the development of UWA communications. Long delay spread, frequency-dependent limited bandwidth and rapid time variation are the main characteristics of UWA channels. The long delay spread results in intersymbol interference (ISI) covering tens to hundreds of symbols and requires complicated equalization at the receiver. The limited bandwidth leads to a relatively low data rate. And the rapid time variation poses a signification challenge to the receiver that needs to track the channels well. As a result, the UWA channels have been regarded as one of the most difficult channels for wireless communications [2].

More serious challenge is exhibited for multiuser UWA communications since there exists the interference signal from other users. Three multiple access techniques, namely frequency division multiple access (FDMA), time division multiple access (TDMA), and code division multiple access (CDMA) are used to reduce the multiple-access interference (MAI). In FDMA scheme [3], [4], the available frequency band is divided into several subbands and assigned to each user. It's not widely used in UWA communications due to the limited bandwidth of UWA channels [5]. The time interval is divided into several time slots and assigned to an individual user in TDMA scheme [6]. The inaccurate synchronization and the low channel utilization caused by the large propagation delay are the main challenges of TDMA scheme [5]. In CDMA scheme, orthogonal spreading codes are assigned to each user. The same time and frequency are shared simultaneously by multiple users in CDMA scheme. In multiuser UWA communications, CDMA is usually more attractive since it can offer the spreading gain and improve immunity against multipath effects at the cost of reducing the data rate of each user [7], [8].

The performance of CDMA scheme for UWA communications have been investigated in multiple studies [8]–[16]. In [8], multichannel equalization with chip hypothesis feedback (CHF) receiver is proposed for CDMA system. The proposed scheme could track the channel variation, which can realize 4 users communications with 12 receivers. A single-element decision feedback equalization (DFE) CDMA receiver which utilizes chip-level adaptive DFE and iterative interference cancellation is proposed in [11]. Experiment results demonstrate the DFE-based CDMA receiver can provide approximately 10^{-5}

Manuscript received June 8, 2019; revised October 20, 2019; accepted January 14, 2020. Date of publication January 17, 2020; date of current version March 12, 2020. This work was supported in part by the National Natural Science Foundation of China under Grants 61801079, 61871418, and 61771396, and in part by the Fundamental Research Funds for the Central Universities DUT18RC(3)018. The review of this article was coordinated by Prof. J. Francisco Paris. *(Corresponding author: Lianyou Jing.)*

L. Jing and H. Yin are with the School of Information and Communication Engineering, Dalian University of Technology, Dalian 116024, China (e-mail: lyjing@dlut.edu.cn; hxyin@dlut.edu.cn).

C. He, H. Wang, and Q. Zhang are with the School of Marine Science and Technology, Northwestern Polytechnical University, Xi'an 710072, China (e-mail: hcb@nwpu.edu.cn; whan@mail.nwpu.edu.cn; zhangqf@nwpu.edu.cn).

Digital Object Identifier 10.1109/TVT.2020.2967429

bit error rate (BER) at 11 dB signal-to-interference-noise ratio (SINR) with 2 or 4 users at an effective rate of 439.5 b/s per user. An interference suppression algorithm using Walsh-Hadamard transform is proposed for DS-CDMA system in [12]. In [14], [15], blind adaptive multiuser detection based on Kalman filter are proposed for moving UWA communications.

Passive time reversal (PTR) technology is also usually adopted for multiuser UWA communications due to it could offer spatial focusing gain [16]–[20]. Meanwhile, the equivalent CIR after PTR is compacted and could be viewed as a sinc function [21]. In [16], a CDAM multiuser system based on the PTR technology is proposed. The SINR is enhanced by utilizing the spatial-temporal processing gain of PTR, and the cochannel interference (CoI) is removed by the approximates-orthogonality of the spreading codes. The processing results of at-sea data demonstrate this system can achieve zero error bits for 8 users with spreading codes of 511 chips.

Recently, interleave-division multiple access (IDMA) [22] is also introduced to UWA communications [11], [23], [24]. Unlike the CDMA scheme, the IDMA system employs the same spreading code for all users. Each user has specific chip interleaver to distinguish with other users. In [11], an IDMA multiuser system is also considered for UWA channels. The experiment results show that IDMA scheme outperforms the CDMA receiver. The elementary signal estimator (ESE) is usually used in IDMA receiver under additive white Gaussian noise (AWGN) and flat fading channels [22]. However, the performance of ESE degrades in multi-path fading channels [25]. In [25], the minimum mean squared error (MMSE) detector is proposed for IDMA system. However, its complexity is much higher than ESE due to channel inverse computation.

The length of spreading codes for UWA comminations is usually large enough to achieve the spreading gain and against the multipath effects. For example, Yang uses m-sequences with 127, 255 and 511 chips in [16]. Consequently, it leads to a very low data rate of the Direct Sequence Spread Spectrum (DSSS) system, especially for bandwidth limited UWA channels. Meanwhile, a user's signal is interference to other users for multiuser communications. That interference is also connected with the number of multipaths. Thus, most of multiuser UWA communications using the DSSS scheme are currently limited to 4 users due to the long delay of UWA channels [16].

To improve the data rate of DSSS system, we introduce cyclic shift keying (CSK) [26] modulation for UWA communications in our early works [27], [28]. The CSK scheme uses the cyclic correlation characteristic of spread spectrum signals. One of cyclically shifted version of the basic sequence at the transmitter represents multiple bits information. Therefore, the CSK modulation is a special M-ary spread spectrum modulation, which a different circular cyclic shift of spreading sequence represents the orthogonal M-ary signal in typical M-ary modulation. CSK modulation is usually used in transform domain communication system (TDCS) [29], [30] and GNSS system [31]. In [30], the authors present a TDCS-IDMA communication system which intergrades the advantage of both OFDM-IDMA and cognitive radio networks with cloud (CRNC). However, the demodulation of CSK is hard decisions which cannot be incorporated with the iteration detection. CSK modulation is specially adapted to UWA communications since it can overcome the spreading gain versus data rate limitations. In [32], we design and test a multiuser CSK system which achieves 40 bits/s/user for 4 users with zero error bits, and 20 bits/s/user for 8 users with low BER.

Based on our previous work [32], we propose a new IDMA scheme with CSK modulation (CSK-IDMA) for multiuser UWA communications in this paper. As compared to existing works, our main contributors are summarized as follow:

1) At the transmitter, the proposed system unitizes CSK modulation to improve the data rate of per user. The improvement of data rate grows with the lengths of spreading code, which is particularly suited to UWA communications systems required high spreading gain to cope with the long delay multipath and the low receive signal to noise ratio (SNR) of UWA channels.
2) At the receiver, the equivalent channel impulse responses (CIR) for each user are compacted by using PTR technique at first. Since the equivalent CIR could be viewed as a sinc function, an ESE could be employed following the PTR to deal with the out of PTR. Meanwhile, PTR also can offer spatial-temporal processing gain to improve the SINR.
3) A soft CSK demodulator based on maximum *a posteriori* (MAP) criterion is proposed based on the output of ESE. The soft decision of CSK demodulation iteratively exchanges extrinsic information with a soft channel decoder to improve overall system performance. The soft output is incorporated into the IDMA system perfectly. Compared with existing multiuser UWA schemes, the proposed scheme can improve the number of users greatly.
4) The proposed CSK-IDMA scheme was tested and verified by collecting experiment data hold in Danjiangkou lake, Henan, China. Data processing results showed that the proposed CSK-IDMA scheme had an excellent performance. It can achieve zero error bits with 8 hydrophones for 8 and 10 users with data rate of 62.5 bits/s/user within 4 kHz bandwidth for 2.3 km transmission and 2.7 km transmission, respectively. For 16 users, it still achieved BER $< 10^{-3}$. To the best of our knowledge, this is the first work which can support more than 8 users for multiuser UWA communications.

The rest of the paper is organized as follows. Section II describes the transmitter and receiver structures of traditional IDMA scheme. Section III gives the transmitter and receiver structure of proposed CSK-IDMA system. Section IV presents simulation results of the proposed CSK-IDMA over UWA channels. Section V presents experiment results of the proposed CSK-IDMA. Finally, Section VI summarizes the conclusions.

II. Conventional IDMA System

We first briefly recall the conventional IDMA system. We consider a synchronous downlink multiple-access system with M users and N receivers. Fig. 1 shows the transmitter and receiver structures of conventional IDMA system. The information bits $\boldsymbol{b}_m$ of m-th user are encoded by a rate R channel encoder which gives coded bits $\boldsymbol{c}_m$. $\boldsymbol{c}_m$ is spread by a length G spreading sequences $\boldsymbol{\alpha} = [\alpha_1, \alpha_2, \ldots, \alpha_G]$, producing the

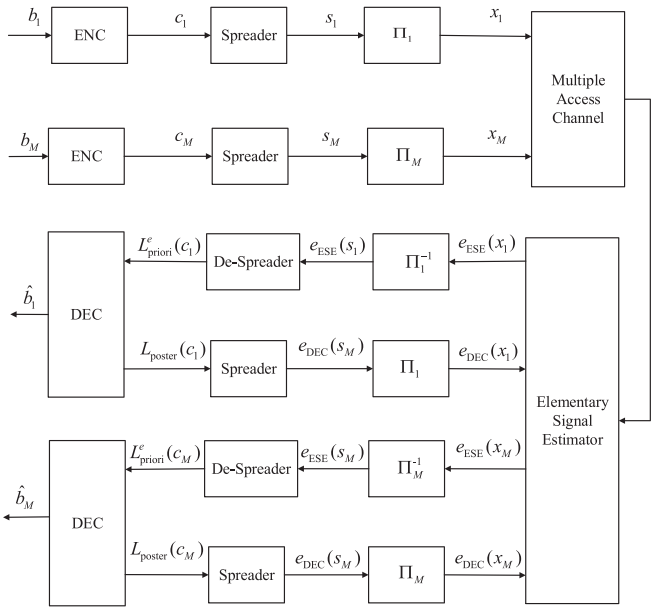

Fig. 1. Transmitter and receiver structures of conventional IDMA scheme with M simultaneous users.

spreading sequence $\boldsymbol{s}_m$. Then, $\boldsymbol{s}_m$ is permutated by a chip interleaver Π_m to get the transmitted symbol $\boldsymbol{x}_m$.

We consider a quasi-static UWA channels of length L. The frequency-selective channel is modeled by a sample space tapped delay line. The discrete time channel between the m-th user and n-th receiver is given as

$$\boldsymbol{h}_{n,m} = [h_{n,m}(0), h_{n,m}(1), \ldots, h_{n,m}(L-1)]^T \tag{1}$$

Then, the discrete time baseband received signal of n-th receiver can be represented by

$$r_n(j) = \sum_{m=1}^{M} \sum_{l=0}^{L-1} h_{n,m}(l) x_m(j-l) + w_n(j) \tag{2}$$

where $w_n(j)$ are samples of an AWGN process with variance $\sigma_n^2 = N_0/2$.

According to (2), the mean and variance of received signal $r_n(j)$ can be represented by

$$\mathrm{E}\left(r_n(j)\right) = \sum_{m=1}^{M} \sum_{l=0}^{L-1} h_{n,m}(l) \mathrm{E}\left(x_m(j-l)\right) \tag{3a}$$

$$\mathrm{Var}\left(r_n(j)\right) = \sum_{m=1}^{M} \sum_{l=0}^{L-1} ||h_{n,m}(l)||^2 \mathrm{Var}\left(x_m(j-l)\right) + \sigma_n^2. \tag{3b}$$

where $\mathrm{E}(\cdot)$ and $\mathrm{Var}(\cdot)$ denote the mean and variance functions, respectively.

Eq. (2) can be rewritten as

$$r_n(j+l) = h_{n,m}(l) x_m(j) + \zeta_{n,m}^{(l)}(j) \tag{4}$$

where $\zeta_{n,m}^{(l)}(j)$ is the interference with respect to m-th user at l-th path for n-th receiver. $\zeta_{n,m}^{(l)}(j)$ can be given by

$$\zeta_{n,m}^{(l)}(j) = r_n(j+l) - h_{n,m}(l) x_m(j) \tag{5}$$

In IDMA scheme, $\zeta_{n,m}^{(l)}(j)$ is approximated as a Gaussian variable based on the central limit theorem. Thus, the condition probability density function (PDF) of $r_n(j+l)$ in (4) can be expressed as

$$P(r_n(j+l)|x_m(j) = \pm 1) = \frac{1}{\sqrt{2\pi \mathrm{Var}\left(\zeta_{n,m}^{(l)}(j)\right)}} \cdot \exp\left(\frac{r(j+l) - \left(\pm h_{n,m}(l) + \mathrm{E}\left(\zeta_{n,m}^{(l)}(j)\right)\right)}{2\mathrm{Var}\left(\zeta_{n,m}^{(l)}(j)\right)}\right)$$

Thus, the extrinsic log-likelihood ratios (LLR) of $x_m(j)$ which is the outputs of ESE in Fig. 1 for n-th receiver signal can be defined as

$$e_{\mathrm{ESE}}^{(n)}(x_m(j)) = \ln \frac{P(\boldsymbol{r}_n|x_m(j) = +1)}{P(\boldsymbol{r}_n|x_m(j) = -1)} \tag{6}$$

where $\ln$ denotes the natural logarithm.

Eq. (6) is related with the statistics information of the interference $\zeta_{n,m}^{(l)}(j)$. We also can obtain the representation of $\mathrm{E}(\zeta_{n,m}^{(l)}(j))$ and $\mathrm{Var}(\zeta_{n,m}^{(l)}(j))$ according to (5),

$$\mathrm{E}\left(\zeta_{n,m}^{(l)}(j)\right) = \mathrm{E}\left(r_n(j+l)\right) - h_{n,m}(l)\mathrm{E}\left(x_m(j)\right) \tag{7a}$$

$$\mathrm{Var}\left(\zeta_{n,m}^{(l)}(j)\right) = \mathrm{Var}(r_n(j+l)) - ||h_{n,m}(l)||^2 \mathrm{Var}(x_m(j)) \tag{7b}$$

The statistics information of $r_n(j+l)$ in (7a) and (7b) are given in (3a) and (3b). And the *a priori* statistics information $\mathrm{E}(x_m(j))$ and $\mathrm{Var}(x_m(j))$ can be obtained by the extrinsic LLR $e_{\mathrm{DEC}}(x_m(j))$, which is the output of channel decoder in previous iteration.

$$\mathrm{E}(x_m(j)) = \tanh(e_{\mathrm{DEC}}(x_m(j)/2)) \tag{8a}$$

$$\mathrm{Var}(x_m(j)) = 1 - (\mathrm{E}(x_m(j)))^2. \tag{8b}$$

Then, the output of the ESE for l-th channel tap is given by

$$e_{\mathrm{ESE}}^{(n)}(x_m(j))_l = \ln \frac{P(r_n(j+l)|x_m(j) = 1)}{P(r_n(j+l)|x_m(j) = -1)} = 2h_{n,m}(l) \frac{r(j+l) - \mathrm{E}\left(\zeta_{n,m}^{(l)}(j)\right)}{\mathrm{Var}\left(\zeta_{n,m}^{(l)}(j)\right)}$$

Assume the inference $\{\zeta_{n,m}^{(0)}(j), \zeta_{n,m}^{(1)}(j), \ldots, \zeta_{n,m}^{(L-1)}(j)\}$ are uncorrelated [22], the extrinsic LLR about $x_m(j)$ is given by

$$e_{\mathrm{ESE}}^{(n)}(x_m(j)) = \sum_{l=0}^{L-1} e_{\mathrm{ESE}}^{(n)}(x_m(j))_l \tag{9}$$

The received signal from multiple receive antennas can be treated as those from a set of independent path [22]. Thus, the

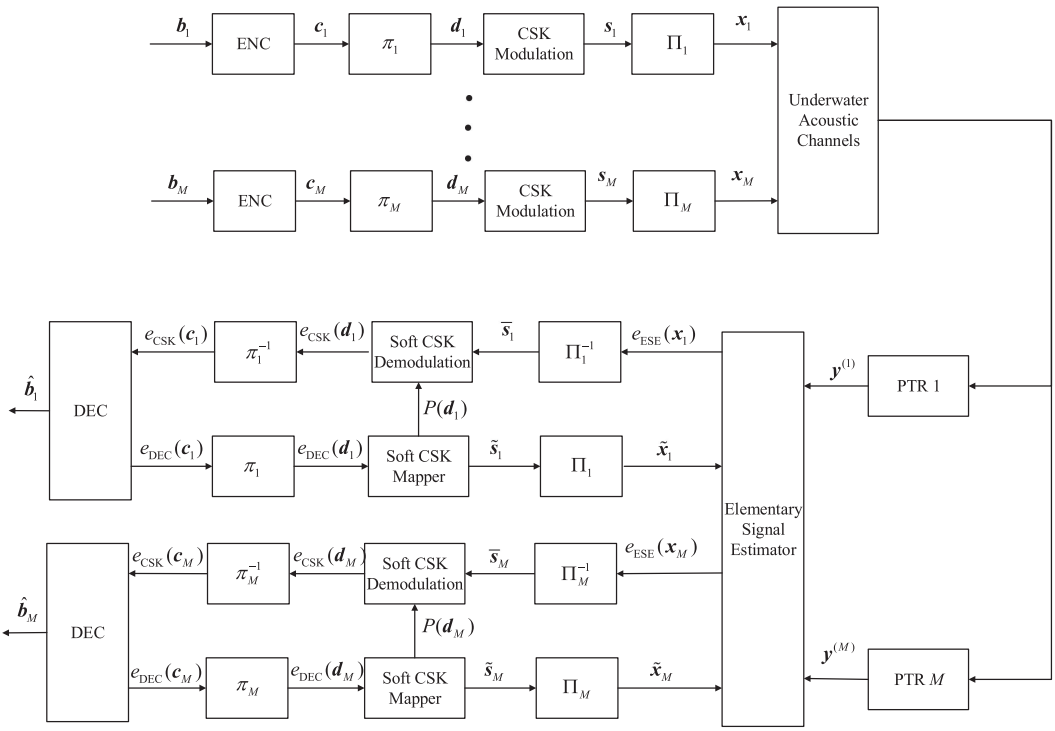

Fig. 2. Transmitter and receiver structures of proposed CSK-IDMA scheme with M simultaneous users.

output of ESE for N receivers is given by

$$e_{\text{ESE}}(x_m(j)) = \sum_{n=1}^{N} e_{\text{ESE}}^{(n)}(x_m(j)) \tag{10}$$

Once we obtain the $e_{\text{ESE}}(x_m(j))$, the extrinsic LLR of $c_m(k)$ is given by

$$\begin{aligned} L_{\text{priori}}^{e}(c_m(k)) &= \sum_{g=1}^{G} \alpha(g) e_{\text{ESE}}(s_m((k-1)G+g)) \\ &= \sum_{g=1}^{G} \alpha(g) e_{\text{ESE}}(x_m(\Pi_m((k-1)G+g))) \end{aligned} \tag{11}$$

A soft decoder is adopted to generate extrinsic information to form an iterative structure. Then, the the extrinsic LLR $L_{\text{priori}}^{e}(c_m(k))$ is inputted into the soft decoder. The output of the soft decoder is the a *posteriori* LLR $L_{\text{poster}}(c_m(k))$. Then, the extrinsic information of DEC output is given by

$$e_{\text{DEC}}(c_m(k)) = L_{\text{poster}}(c_m(k)) - L_{\text{priori}}^{e}(c_m(k)) \tag{12}$$

$e_{\text{DEC}}(c_m(k))$ can be used for computing the *a priori* statistics information $\text{E}(x_m(j))$ and $\text{Var}(x_m(j))$ in (8a) and (8b). In this way, the receiver realizes iterative detection. The iteration stops if the receiver decodes all information successfully or reaches the maximum iterations.

III. Proposed CSK-IDMA System

A main disadvantage of DSSS system is that the data rate is quite low, especially in the bandwidth limited UWA channels. Thus, we apply a high bandwidth efficiency modulation, CSK modulation, to improve the data rate in this paper.

The transmitter and receiver structures of CSK-IDMA are presented in Fig. 2. At the transmitter, there are two differences compared with conventional IDMA system. The first one is that the CSK modulation instead of DSSS to improve the data rate. The second one is that there are two interleavers in CSK-IDMA scheme. The information bits are first encoded by channel encoder, which is the same as the conventional IDMA system. Then, the encoded bit $\boldsymbol{c}_m$ is permutated by a random bit interleaver π_m, producing the interleaved and encoded bit sequence $\boldsymbol{d}_m$. This bit interleaver π_m is used to disperse the bit errors caused by the CSK misjudgment since one CSK symbol can transmit multiple bits. The chip interleaver Π_m is used to distinguish users which is the key principle of IDMA scheme.

At the receiver, there are also two differences compared with IDMA system. The first one is that we utilize the PTR technique. The PTR processing can achieve spatial and temporal focusing for the desired user, while can not achieve the same effect for the other interference users. Thus, the PTR processing can improve the SINR. Additionally, the equivalent CIR after PTR processing could be viewed as sinc function, we could use the ESE following the PTR processing to avoid the the complexity of MMSE detector. For each user, the PTR processing turns the single-input multiple-output (SIMO) system into an equivalent single-input single-output (SISO) system. And the equivalent channel is shorten than original channels. The second one is that the proposed scheme utilizes two layer of iterative processing: the inner-layer iteration is the soft CSK demodulation combines with the soft channel decoder to form an iterative structure for

each user, the outer-layer iteration is for multiuser detection (MUD).

A. CSK Modulation

In conventional DSSS system, a spreading sequence $\boldsymbol{\alpha}$ with G chips presents only one bit (for BPSK modulation). Thus, the data rate of DSSS scheme is

$$R_{\text{DSSS}} = \frac{1}{GT_c} \tag{13}$$

where T_c is the duration of chip.

For CSK modulation, information is represented by the value of cyclically shifted of the spreading sequence. We define a circular shift matrix $\boldsymbol{T}$ to mathematically represent the shifting process,

$$\boldsymbol{T} = \begin{bmatrix} \mathbf{0}_{1\times(G-1)} & 1 \\ \boldsymbol{I}_{G-1} & \mathbf{0}_{(G-1)\times 1} \end{bmatrix} \tag{14}$$

The vector will be circular shift by 1 to right if it multiplies by matrix $\boldsymbol{T}$. Then, vector $\boldsymbol{T}^g\boldsymbol{\alpha}$ is the form of an original spreading sequence $\boldsymbol{\alpha}$ circularly shifted by g chips. Thus, a spreading sequence can presents $Q = \ln G$ bits. The data rate of CSK is

$$R_{\text{CSK}} = \frac{Q}{GT_c} = \frac{\ln G}{GT_c} \tag{15}$$

It can improve the bandwidth efficiency dramatically. And the improvement of data rate is related with the length of spreading sequence G. Then, it overcomes the spreading gain versus data rate limitations.

In CSK scheme, the information bits are first segmented into groups of length Q. Translate the Q bits into decimalism, which is denoted by Δ, $0 \le \Delta \le 2^Q - 1$. Then, the modulated CSK symbol is given by

$$\boldsymbol{s} = \boldsymbol{T}^{\Delta}\boldsymbol{\alpha} \tag{16}$$

At the receiver, the demodulation of CSK symbol is also implemented by using a correlator which is similar with DSSS system. The output of correlator can be calculated by using the Fast Fourier Transform (FFT) to minimize the computational complexity. Then, the autocorrelation result of spreading sequence $\boldsymbol{\alpha}$ can be expressed as

$$\boldsymbol{\vartheta}_{\boldsymbol{\alpha}} = \frac{1}{G}\text{Real}\{\boldsymbol{F}^{-1}((\boldsymbol{F}\boldsymbol{\alpha})^* \odot (\boldsymbol{F}\boldsymbol{\alpha}))\} \tag{17}$$

where $\boldsymbol{F}$ is Fourier transform matrix, $\odot$ denotes Hadamard product, $(\cdot)^*$ represents the conjugate, Real$\{x\}$ denotes the real part of x. Since we adopt the BPSK modulation in our CSK system, only the data on the real part is useful. The element of $\boldsymbol{\vartheta}_{\boldsymbol{\alpha}}$ is given as

$$\vartheta_{\boldsymbol{\alpha}}(g) = \begin{cases} 1, & g = 1 \\ \varpi_g, & \text{otherwise} \end{cases} \tag{18}$$

where $\varpi_g \ll 1$.

Then, the output of CSK demodulator can be expressed as

$$\boldsymbol{\theta} = \frac{1}{G}\text{Real}\{\boldsymbol{F}^{-1}((\boldsymbol{F}\hat{\boldsymbol{s}})^* \odot (\boldsymbol{F}\boldsymbol{\alpha}))\} \tag{19}$$

where $\hat{\boldsymbol{s}}$ is the estimation of $\boldsymbol{s}$.

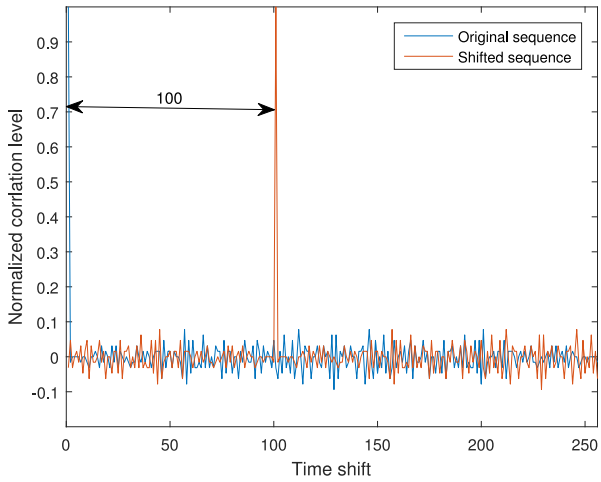

Fig. 3. Correlation results of original sequence and shifted sequence.

According to the autocorrelation property of spreading sequence, $\boldsymbol{\theta}$ can be given as

$$\boldsymbol{\theta} = \boldsymbol{T}^{\Delta}\boldsymbol{\vartheta}_{\boldsymbol{\alpha}} \tag{20}$$

The element of $\boldsymbol{\theta}$ is given as

$$\theta(g) = \begin{cases} \vartheta_{\boldsymbol{\alpha}}(g-\Delta), & g > \Delta \\ \vartheta_{\boldsymbol{\alpha}}(G-(g-\Delta)), & g \le \Delta \end{cases} \tag{21}$$

Namely, the shifting processing does not change the autocorrelation property of spreading sequence. It only changes the peak position. Thus, the demodulation of CSK system is based on the position of the correlation output peak. Fig. 3 shows the correlation results of original sequence and shifted sequence. The length of spreading sequence is 256. The number of shifted chips is $\Delta = 100$. From the figure, we find the peak location of correlation for shifted sequence also shifts 100.

Hence, we can obtain the estimation of cyclic shifted information $\hat{\Delta}$ through searching the peak position of $\boldsymbol{\theta}$.

$$\hat{\Delta} = \arg\max_{g} \boldsymbol{\theta} \tag{22}$$

The original bit information can be obtained by translating $\hat{\Delta}$ into binary.

B. PTR Processing

One of main characteristic of UWA channels is that channel delay is very long. In such channels, the ISI can even over hundreds of transmitted symbols. The interference from other users are more serious in this situation. Thus, we first use PTR technique to compress the channels. Meanwhile, PTR technique also provides the spatial-temporal processing gain to improve SINR.

Assume that $\hat{h}_{n,m}(t)$ is the channel estimation result. Then, the output of the PTR processing for the i-th user is given as

$$\begin{aligned} y^{(i)}(t) &= \sum_{n=1}^{N} r_n(t) \otimes \hat{h}_{n,i}(-t) \\ &= \sum_{n=1}^{N} \left[\sum_{m=1}^{M} x_m(t) \otimes h_{n,m}(t) + w_n(t) \right] \otimes \hat{h}_{n,i}(-t) \end{aligned}$$

$$
\begin{aligned}
&= x_i(t) \otimes \sum_{n=1}^{N} h_{n,i}(t) \otimes \hat{h}_{n,i}(-t) \\
&\quad + \left[\sum_{m=1, m\neq i}^{M} x_m(t) \otimes \sum_{n=1}^{N} h_{n,m}(t) \otimes \hat{h}_{n,i}(-t) \right] \\
&\quad + \sum_{n=1}^{N} w_n(t) \otimes \hat{h}_{n,i}(-t) \\
&= x_i(t) \otimes Q_{i,i}(t) + \sum_{m=1, m\neq i}^{M} x_m(t) \otimes Q_{m,i}(t) + \tilde{w}_i(t)
\end{aligned} \tag{23}
$$

where $\otimes$ denotes the convolution operation and

$$Q_{m,i}(t) = \sum_{n=1}^{N} h_{n,m}(t) \otimes \hat{h}_{n,i}(-t) \tag{24}$$

$$\tilde{w}_i(t) = \sum_{n=1}^{N} w_n(t) \otimes \hat{h}_{n,i}(-t) \tag{25}$$

In (23), the first term is the desire signal and $Q_{i,i}(t)$ is the equivalent channel for i-th user after PTR processing. The second term is the inference signal and $Q_{m,i}(t)$ is the equivalent inference channel from m-th user with respect to i-th user. $\tilde{w}_i(t)$ is the noise with variance $\tilde{\sigma}_i^2 = \sum_{l=0}^{L-1} ||\hat{h}_{n,i}(l)||^2 \sigma_n^2$.

As shown in [21], the equivalent CIR $Q_{i,i}(t)$ is compacted and could be viewed as a sinc function. Thus, we could use the ESE to deal with the output of PTR processing directly. Additionally, the gain of $Q_{i,i}(t)$ is much larger than others $Q_{m,i}(t)$ $(m \neq i)$. It also improves the SINR of each user.

Generally speaking, the length of equivalent channel $Q_{i,i}$ is $\tilde{L} = L + \hat{L} - 1$, which $\hat{L}$ is the length of estimated channel $\hat{h}_{n,i}(t)$. However, the primary paths of $Q_{i,i}$ are concentrated around $\tilde{l} = \hat{L} - 1$ due to the compressive characteristic of PTR processing. Thus, the output of PTR processing can be rewritten as

$$y^{(i)}(j) = \sum_{m=1}^{M} \sum_{l=0}^{\tilde{L}} Q_{m,i}(l) x_m(j-l) + \tilde{w}_i(j). \tag{26}$$

Then, the PTR processing turns the SIMO system into an equivalent SISO system.

C. Elementary Signal Estimator

The elementary signal estimator of proposed receiver is similar with the conventional IDMA system. The difference is that the input signal is different for each user. $y^{(i)}(j)$ is just for i-th user. Then, the statistics information for i-th user can be obtained by

$$\mathrm{E}(y^{(i)}(j)) = \sum_{m=1}^{M} \sum_{l=0}^{\tilde{L}-1} Q_{m,i}(l) \mathrm{E}(x_i(j-l)) \tag{27a}$$

$$\mathrm{Var}(y^{(i)}(j)) = \sum_{m=1}^{M} \sum_{l=0}^{\tilde{L}-1} ||Q_{m,i}(l)||^2 \mathrm{Var}(x_i(j-l)) + \sum_{n=1}^{N} \sum_{l=0}^{\tilde{L}-1} ||\hat{h}_{n,i}(l)||^2 \sigma_n^2 \tag{27b}$$

$$\mathrm{E}(\zeta_i^{(l)}(j)) = \mathrm{E}(y^{(i)}(j+l)) - Q_{i,i}(l) \mathrm{E}(x_i(j)) \tag{27c}$$

$$\mathrm{Var}(\zeta_i^{(l)}(j)) = \mathrm{Var}(y^{(i)}(j+l)) - ||Q_{i,i}(l)||^2 \mathrm{Var}(x_i(j)) \tag{27d}$$

And the LLR of $x_i(j)$ is given by

$$e_{\mathrm{ESE}}(x_i(j))_l = 2Q_{i,i}(l) \frac{y^{(i)}(j+l) - \mathrm{E}\left(\zeta_i^{(l)}(j)\right)}{\mathrm{Var}\left(\zeta_i^{(l)}(j)\right)} \tag{28}$$

To compute (28), we need to know the statistic information $\mathrm{E}(x_i(j))$ and $\mathrm{Var}(x_i(j))$. At the first iteration, $\mathrm{E}(x_i(j)) = 0$ and $\mathrm{Var}(x_i(j)) = 1$. And they can be obtained by the output of decoder in the next iterations.

Since the PTR technique could compress the channel, the gain of main path is much larger than that of other pathes. Different (10), the LLR of $x_i(j)$ is approximated by

$$e_{\mathrm{ESE}}(x_i(j)) \approx e_{\mathrm{ESE}}(x_i(j))_{\breve{l}} \tag{29}$$

where $\breve{l}$ is corresponding to the main path of the equivalent channel.

D. Inner-Layer Iteration With Soft CSK Demodulation

After deinterleaving, the output of deinterleaver Π_i^{-1} is $e_{\mathrm{ESE}}(s_i(j))$. Grouping the signals $e_{\mathrm{ESE}}(s_i(j))$ according to the length of the spreading sequence G. Then, we can obtain the mean of $s_i(g)$ according to (8a). Let $\bar{s}_i(g)$ denote the mean of $s_i(g)$. Then,

$$\bar{s}_i(g) = \mathrm{E}(s_i(g)) = \tanh(e_{\mathrm{ESE}}(s_i(g)/2)) \tag{30}$$

It is worth noting that although $\bar{\boldsymbol{s}}_i$ is the mean of the signal $\boldsymbol{s}_i$, it can still be regarded as a CSK signal with noise. Thus, the soft estimation of $\bar{\boldsymbol{s}}_i$ can be seen as the sum of desire signal $\boldsymbol{s}_i$ and a random disturbance variable $\boldsymbol{\epsilon}_i$.

$$\bar{s}_i(g) = s_i(g) + \epsilon_i(g) \tag{31}$$

where $\boldsymbol{\epsilon}_i$ is a Gaussian noise with zero mean and variance $\bar{\sigma}_i^2$. And the disturbance variance $\bar{\sigma}_i^2$ can be estimated by:

$$\bar{\sigma}_i^2 = \frac{1}{G} \sum_{g=1}^{G} 1 - ||\bar{s}_i(g)||^2 \tag{32}$$

Using the soft estimation $\bar{\boldsymbol{s}}_i$ to demodulate the CSK signal, the output of correlator is given by

$$\boldsymbol{\theta}_i = \frac{1}{G} \mathrm{Real}\{\boldsymbol{F}^{-1}((\boldsymbol{F}\bar{\boldsymbol{s}}_{\boldsymbol{i}})^* \odot (\boldsymbol{F}\boldsymbol{\alpha}))\} \tag{33}$$

There are two factors which affects the value $\theta_i(g),\ g \neq \Delta$. The first one is the autocorrelation characteristic of sequence $\boldsymbol{\alpha}$, which is affected by the sidelobe of the autocorrelation. However, the level of sidelobe is fixed once $\boldsymbol{\alpha}$ is determined. And it can be computed in advance. The second factor is the

disturbance variable $\boldsymbol{\epsilon}_i$. Thus, $\theta_i(g)$ can be represented by

$$\theta_i(g) = \begin{cases} 1 + \upsilon_g, \ g = \Delta, \\ \varpi_g + \upsilon_g, \ \text{others}, \end{cases} \tag{34}$$

where Δ is the shifting size which represents the information, υ_g is caused by the disturbance variable $\boldsymbol{\epsilon}_i$, which is a Gaussian variable with zero mean and variance $\sigma^2_{\boldsymbol{\epsilon}_i} = \bar{\sigma}^2_i / G$. To reduce the complexity, we assume that ϖ_g is also a Gaussian variable with zero mean and variance $\sigma^2_{\boldsymbol{\alpha}}$. $\sigma^2_{\boldsymbol{\alpha}}$ can be computed according to the result of autocorrelation. Thus, the variance of $\theta_i(g)$ is

$$\sigma^2_{\boldsymbol{\theta}_i} = \begin{cases} \sigma^2_{\boldsymbol{\epsilon}_i}, \ g = \Delta, \\ \sigma^2_{\boldsymbol{\alpha}} + \sigma^2_{\boldsymbol{\epsilon}_i}, \ \text{others}, \end{cases} \tag{35}$$

The peak location of $\boldsymbol{\theta}_i$ represents the information according to (34). We can demodulate the information by searching the peak location, which is the classical hard demodulation.

In this paper, we adopt soft demodulation in order to improve the performance. Assume $\boldsymbol{d}_i = [d_i(1), d_i(2), \ldots, d_i(Q)]^T$ denote the coded information bits which are mapped by CSK signal of $\bar{\boldsymbol{s}}_i$. Let $\boldsymbol{d}_i^{\Delta}$ denote the bit sequence which the value converted to decimal is $\Delta, 0 \le \Delta \le 2^Q - 1$. And the corresponding CSK signal is $\boldsymbol{s}_i^{\Delta}$. According to (34) and (35), the PDF of $\theta_i(g)$ is given by

$$P(\theta_i(g)|\boldsymbol{s}_i = \boldsymbol{s}_i^{\Delta}) = \begin{cases} \frac{1}{\sqrt{2\pi\sigma^2_{\boldsymbol{\epsilon}_i}}} \exp\left(-\frac{(\theta_i(g)-1)^2}{2\sigma^2_{\boldsymbol{\epsilon}_i}}\right), \ g = \Delta, \\ \frac{1}{\sqrt{2\pi(\sigma^2_{\boldsymbol{\alpha}}+\sigma^2_{\boldsymbol{\epsilon}_i})}} \exp\left(-\frac{(\theta_i(g))^2}{2(\sigma^2_{\boldsymbol{\alpha}}+\sigma^2_{\boldsymbol{\epsilon}_i})}\right), \ \text{others}, \end{cases} \tag{36}$$

Assume the components of $\boldsymbol{\theta}_i$ are independent, then,

$$\begin{aligned} P(\boldsymbol{\theta}_i|\boldsymbol{d}_i = \boldsymbol{d}_i^{\Delta}) &= \prod_{g=1}^{G} P(\theta_i(g)|\boldsymbol{d}_i = \boldsymbol{d}_i^{\Delta}) \\ &= \prod_{g=1}^{G} P(\theta_i(g)|\boldsymbol{s}_i = \boldsymbol{s}_i^{\Delta}) \end{aligned} \tag{37}$$

According to (36),

$$\begin{aligned} P(\boldsymbol{\theta}_i|\boldsymbol{d}_i = \boldsymbol{d}_i^{\Delta}) &= \frac{1}{\sqrt{2\pi\sigma^2_{\boldsymbol{\epsilon}_i}}} \left(\frac{1}{\sqrt{2\pi(\sigma^2_{\boldsymbol{\alpha}} + \sigma^2_{\boldsymbol{\epsilon}_i})}}\right)^{G-1} \\ &\quad \cdot \exp\left(-\frac{\sum_{g=1, g\neq\Delta}^{G}(\theta_i(g))^2}{2(\sigma^2_{\boldsymbol{\alpha}} + \sigma^2_{\boldsymbol{\epsilon}_i})} - \frac{(\theta_i(\Delta) - 1)^2}{2\sigma^2_{\boldsymbol{\epsilon}_i}}\right) \\ &= \Lambda \exp\left(\frac{(\theta_i(\Delta))^2}{2(\sigma^2_{\boldsymbol{\alpha}}+\sigma^2_{\boldsymbol{\epsilon}_i})} - \frac{(\theta_i(\Delta))^2}{2\sigma^2_{\boldsymbol{\epsilon}_i}} + \frac{\theta_i(\Delta)}{\sigma^2_{\boldsymbol{\epsilon}_i}}\right) \end{aligned} \tag{38}$$

where

$$\begin{aligned} \Lambda &= \frac{1}{\sqrt{2\pi\sigma^2_{\boldsymbol{\epsilon}_i}}} \left(\frac{1}{\sqrt{2\pi(\sigma^2_{\boldsymbol{\alpha}} + \sigma^2_{\boldsymbol{\epsilon}_i})}}\right)^{G-1} \\ &\quad \cdot \exp\left(-\frac{\sum_{g=1}^{G}(\theta_i(g))^2}{2(\sigma^2_{\boldsymbol{\alpha}} + \sigma^2_{\boldsymbol{\epsilon}_i})} - \frac{1}{\sigma^2_{\boldsymbol{\epsilon}_i}}\right) \end{aligned}$$

Λ is constant for specified $\boldsymbol{\theta}_i$.

The extrinsic LLR of coded bit $d_i(q)$ is given as

$$e_{\text{CSK}}(d_i(q)) = L_{\text{poster}}(d_i(q)) - L_{\text{priori}}(d_i(q)) \tag{39}$$

where $L_{\text{priori}}(d_i(q))$ is the *a priori* information,

$$L_{\text{priori}}(d_i(q)) = \ln \frac{P(d_i(q) = 0)}{P(d_i(q) = 1)} \tag{40}$$

At the first inner-layer iteration, the *a priori* information is zero.

The *a posteriori* LLR is given by

$$\begin{aligned} L_{\text{poster}}(d_i(q)) &= \ln \frac{P(d_i(q) = 0|\boldsymbol{\theta}_i)}{P(d_i(q) = 1|\boldsymbol{\theta}_i)} \\ &= \ln \frac{\sum_{\forall \boldsymbol{d}_i : d_i(q)=0} P(\boldsymbol{\theta}_i|\boldsymbol{d}_i) P(\boldsymbol{d}_i)}{\sum_{\forall \boldsymbol{d}_i : d_i(q)=1} P(\boldsymbol{\theta}_i|\boldsymbol{d}_i) P(\boldsymbol{d}_i)} \end{aligned} \tag{41}$$

Then, (41) can be rewritten as

$$L_{\text{poster}}(d_i(q)) = \ln \frac{\sum_{\forall \Delta, \boldsymbol{d}_i : d_i(q)=0} \exp\left(\frac{(\theta_i(\Delta))^2}{2(\sigma^2_{\boldsymbol{\alpha}}+\sigma^2_{\boldsymbol{\epsilon}_i})} - \frac{(\theta_i(\Delta))^2}{2\sigma^2_{\boldsymbol{\epsilon}_i}} + \frac{\theta_i(\Delta)}{\sigma^2_{\boldsymbol{\epsilon}_i}}\right) P(\boldsymbol{d}_i)}{\sum_{\forall \Delta, \boldsymbol{d}_i : d_i(q)=1} \exp\left(\frac{(\theta_i(\Delta))^2}{2(\sigma^2_{\boldsymbol{\alpha}}+\sigma^2_{\boldsymbol{\epsilon}_i})} - \frac{(\theta_i(\Delta))^2}{2\sigma^2_{\boldsymbol{\epsilon}_i}} + \frac{\theta_i(\Delta)}{\sigma^2_{\boldsymbol{\epsilon}_i}}\right) P(\boldsymbol{d}_i)} \tag{42}$$

$P(\boldsymbol{d}_i)$ is computed according to the a *priori* probability of coded bit. It can be calculated as

$$P\left(\mathbf{d}_i = \mathbf{d}_i^{\Delta}\right) = \frac{\prod_{q=1}^{Q} P\left(d_i(q) = d_i^{\Delta}(q)\right)}{\sum_{\Delta=1}^{G} \prod_{q=1}^{Q} P\left(d_i(q) = d_i^{\Delta}(q)\right)}. \tag{43}$$

We remove those combinations in (43) which cannot be mapped into a CSK symbol to improve the soft decision.

Right now, we realize the soft demodulation of CSK signal and compute the extrinsic LLR $e_{\text{CSK}}(d_i(q))$ according to (39), (40), (42) and (43).

Once we obtain the extrinsic LLR $e_{\text{CSK}}(d_i(q))$, we deliver it into the soft channel decoder after deinterleaving. The soft channel decoder then treats them as priors. The channel decoding of our system is the same with conventional IDMA system and it is a mature technology, whose details are omitted here. The soft decoder generates extrinsic information $P(d_i(q))$, which is fed back to soft CSK demodulation as the prior information for the next iteration. In this way, the inner-layer iteration is realized. The iteration can stop when the channel decoder successfully decodes or reach the max iterations.

E. Outer-Layer Iteration

After the inner-layer iteration, we already obtain the probability of CSK symbols $P(\boldsymbol{d}_i)$ and the soft CSK symbol $\tilde{\boldsymbol{s}}_{\boldsymbol{i}}$. The probability $P(\tilde{s}_i(g) = 1)$ is then calculated from the probability of CSK signal $P(\tilde{\boldsymbol{s}}_i)$ via

$$\begin{aligned} P(\tilde{s}_i(g) = 1) &= \sum_{\Delta=1}^{G} \gamma_{\Delta} P(\tilde{\boldsymbol{s}}_i = \boldsymbol{s}_i^{\Delta}) \\ &= \sum_{\Delta=1}^{G} \gamma_{\Delta} P(\boldsymbol{d}_i = \boldsymbol{d}_i^{\Delta}) \end{aligned} \tag{44}$$

Algorithm 1: Proposed Algorithm.

for each $i \in [1, M]$ **do**
  PTR processing for i-th user to obtain $y^{(i)}(t)$;
  Initialize the *a priori* information $P(d_i = 1) = \frac{1}{2}$, $\mathrm{E}(x_i(j)) = 0$, and $\mathrm{Var}(x_i(j)) = 0$;
end for
for $i_{\text{outer}} = 1$; $i_{\text{outer}} < N_{\text{outer}}$; $i_{\text{outer}} + +$ **do**
  for each $i \in [1, M]$ **do**
    Calculate the $e_{\text{ESE}}(x_i(j))$;
    Calculate the mean of $s_i(g)$.
    Calculate the correlation result $\boldsymbol{\theta}_i$;
    for $i_{\text{inner}} = 1$; $i_{\text{inner}} < N_{\text{inner}}$; $i_{\text{inner}} + +$ **do**
      Calculate the *a priori* information $L_{\text{priori}}(d_i(q))$;
      Calculate the *a posteriori* information $L_{\text{poster}}(d_i(q))$;
      Calculate the extrinsic LLR $e_{\text{CSK}}(d_i(q))$;
      Input $e_{\text{CSK}}(d_i(q))$ to the soft decoder after de-interleaving to obtain the extrinsic information $P(d_i(q))$.
    end for
    Calculate the $\mathrm{E}(x_i(j))$ and $\mathrm{Var}(x_i(j))$;
  end for
end for

where

$$\gamma_\Delta = \begin{cases} 0, & s_i^\Delta(g) = 0; \\ 1, & s_i^\Delta(g) = 1; \end{cases} \tag{45}$$

Due to $\boldsymbol{x}_i$ is permutation of $\boldsymbol{s}_i$, then,

$$\begin{aligned} \tilde{x}_i(j) &= \mathrm{E}(x_i(j)) = P(x_i(j) = 1) - P(x_i(j) = -1) \\ &= P(\tilde{s}_i(\Pi_i(j)) = 1) - P(\tilde{s}_i(\Pi_i(j)) = -1) \end{aligned} \tag{46a}$$

$$\mathrm{Var}(x_i(j)) = 1 - (\mathrm{E}(x_i(j)))^2. \tag{46b}$$

The $\mathrm{E}(x_i(j))$ and $\mathrm{Var}(x_i(j))$ could be used in (27a)–(27d) as the input of ESE in the next outer-layer iteration.

Based on the above discussions, the proposed receiver in this paper is summarized in Algorithm 1. N_{outer} and N_{inner} denote the maximum iteration number of inner-layer iteration and outer-layer iteration, respectively.

IV. Simulation

In this section, we verify the performance of the proposed system over quasi-static UWA channels through Monte Carlo simulations. There are 8 users and 8 receivers. The length of spreading sequence is 256. Thus, one sequence presents $Q = \ln 256 = 8$ bits. We consider a rate $1/2$ convolutional code. Two independent interleavers are employed by each user at the transmitter. The simulated channels are sparse with spread delay $L = 100$, where $N_p = 15$ among them are active. The amplitudes of paths follow Rayleigh distributed. The average power of paths are decreasing exponentially with the delay, where the gain is 20 dB between the first path and the last path. The channel gain for is normalized for each user. Then, the power of receive signal for each user is the same. We adopt MMSE-based channel estimation algorithm to estimate the channels.

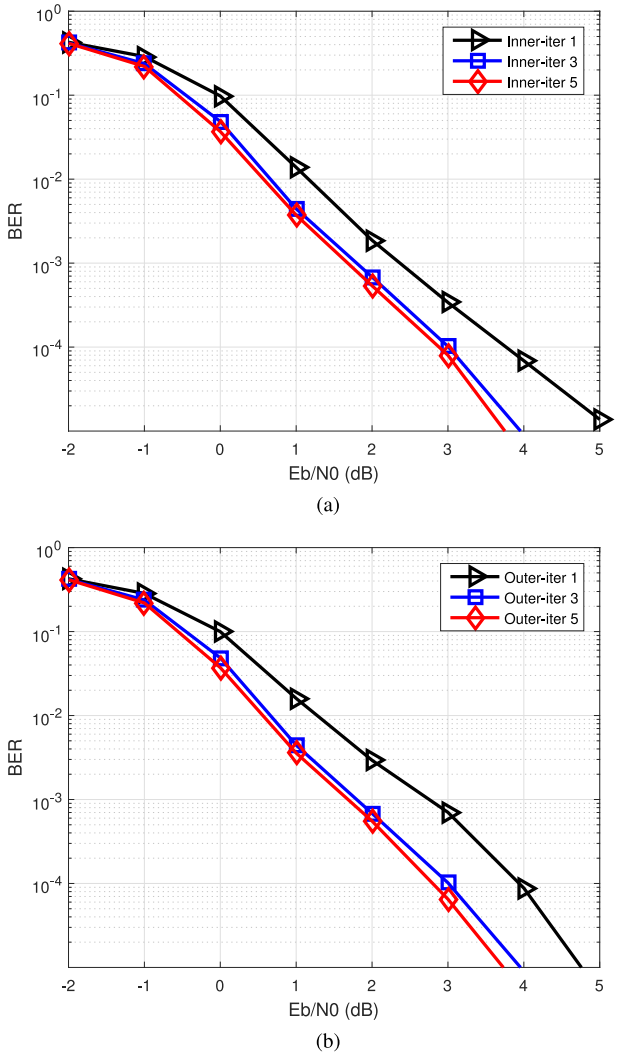

Fig. 4. The impact of the number of iterations. (a) Inner-layer iteration. (b) Outer-layer iteration.

We first study the impact of the number of iterations. Fig. 4 gives the impact of the number of inner-layer iterations with 3 outer-layer iterations (Fig. 4(a)) and the impact of the number of outer-layer iterations with 3 inner-layer iterations (Fig. 4(b)). From Fig. 4, we see that the BER performance improves as the number of iterations increases. But the performance gain decreases as the number of iterations increases. According to Fig. 4, 3 iteration is a good choice for both inner-layer and outer-layer by considering the tradeoff between complexity and BER performance.

As mentioned above, the performance of proposed scheme relies on the sidelobe of the autocorrelation. Thus, we also simulate the BER performance of different spreading sequences. We test 3 PN codes: two *m* sequences and one *small Kasami* sequence [33]. The two *m* sequences are denoted by *lse-ao-m255* and *co-msqcc-m255*, respectively. And *mse-ao-sk255* is the *small Kasami* sequence. The *lse-ao*, *co-msqcc* and *mse-ao*

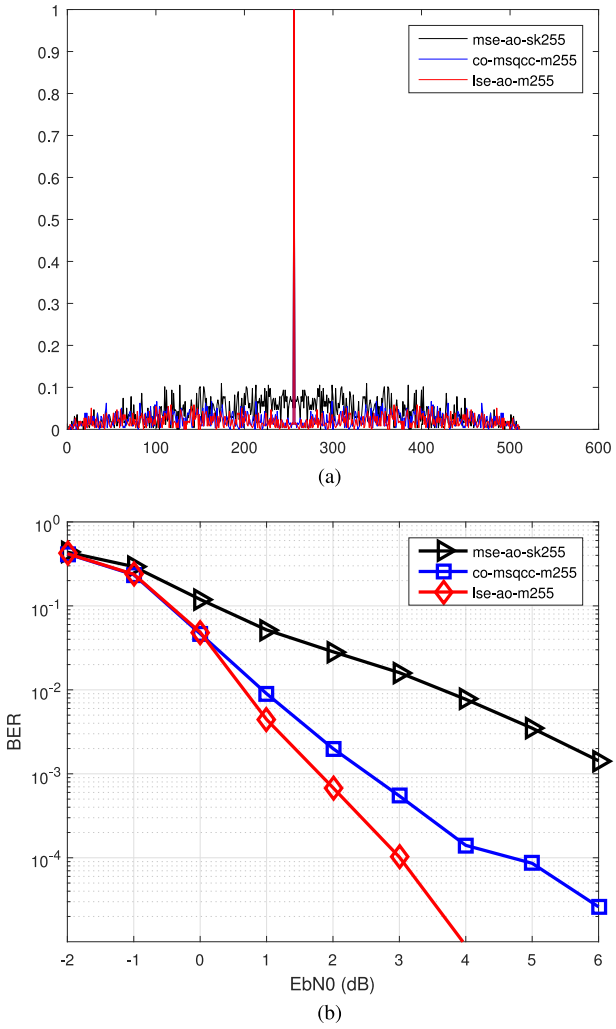

Fig. 5. The impact of spreading sequences. (a) The correlation results of different spreading sequences. (b) The BER results with different spreading sequences.

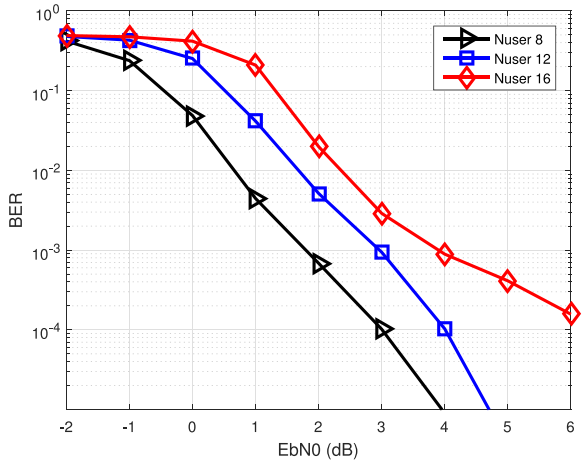

Fig. 6. The BER performance for different users.

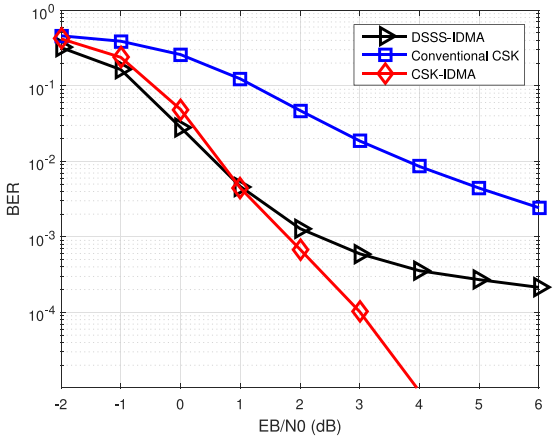

Fig. 7. Performance comparison of the proposed scheme with DSSS-IDMA scheme and conventional CSK scheme.

are represented the least side-lobe energy auto-optimal (LSE-AO), the cross-optimal minimum mean-square cross-correlation (CO-MSQCC) and the maximum side-lobe energy auto-optimal (MSE-AO) phase optimization criteria are adopted to generate the PN codes. More details could be obtained in [33] and references therein. Fig. 5(a) shows the correlation results of different spreading sequences. It can be seen that the *lse-ao-m255* has the lowest sidelobe. The sidelobe of *mse-ao-sk255* is the highest. The variance of the sidelobe for *mse-ao-sk255*, *co-msqcc-m255* and *lse-ao-m255* are 0.0050, 0.0016 and 0.0011, respectively. Fig. 5(b) gives the BER performance for corresponding spreading sequences. The performance of which uses *lse-ao-m255* has the best BER performance. The performance difference between different spreading codes is very huge. Thus, our proposed scheme is sensitive to the the sidelobe of the autocorrelation of spreading sequences.

Fig. 6 shows the BER performance for different users. It is obvious that the inter-user interference increases as the number of users increases, especially for long-delay UWA channels. Naturally, as the number of users increases, the BER increases. The performance loss caused by adding 4 users is about 1 dB.

We also compare the BER performance with conventional DSSS-IDMA scheme and conventional CSK system. The PTR processing are is adopted for DSSS-IDMA scheme [16] and conventional CSK system [32]. Because DSSS system and CSK system have different rate under the same spreading sequence, we evaluate the BER performance under the same data rate and the same received SNR. Then, the length of spreading sequence for DSSS system is 32. Fig 7 shows the comparison result. From this figure, we find the performance of CSK-IDMA scheme is similar to that of DSSS-IDMA scheme at low SNR. However, the superiority of CSK-IDMA scheme is obvious in the case of high SNR. Compared with conventional-CSK system, the proposed CSK-IDMA scheme can greatly improve the BER performance since we adopt soft decision and MUD based on ESE.

V. Lake Experiment Results

A. Experiment Setup

In this section, we employ the data collected from a lake experiment to verify the performance of the proposed scheme.

Fig. 8. The experiment location in google earth.

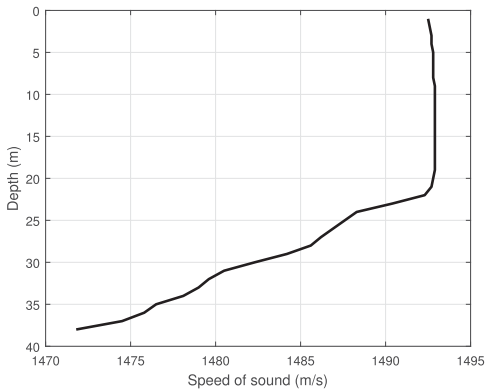

Fig. 9. The sound speed curve in experimental area.

This experiment was held in the area of Danjiangkou lake, Henan, China, on Sept. 26, 2018. Location of the experiment is shown in Fig. 8. The transmitter boat and receiver boats are mainly at the centre of the lake and there is no blocking. During the experiment, the wind and waves are small. The bottom of the lake is the sediment. We used bathythermograph to measure the temperature and depth of the experimental area. In the experimental area, the water depth was approximately 40 m. And we also computed the sound speed in the experimental area according to the temperature and depth, as shown in Fig. 9. This sound speed introduced a downward refractive channel with a thermocline at a depth about 23 m. The transducer was deployed at 20 m below the surface. The location of transducer was on the edge of the thermocline. The source level of the transducer was about 181 dB re μPa. Two receiving arrays were located at a distance of 2.3 km (marked as node 1) and 2.7 km (marked as node 2), which each array has 8 vertically placed hydrophones with a uniform-spacing of 0.25 m between adjacent elements.

The carrier frequency and bandwidth of transmitted signals were $f_c = 6$ kHz and $B = 4$ kHz, respectively. The sampling rate of passband signals was 48 kHz. We used the square root raised cosine pulse with a roll-off factor 0.25 to perform as the pulse shaping filter. The length of the spreading sequence was 256 chips, and it can represent $Q = 8$ coded bits. The spreading sequence was formed by adding 1 at the end of *lse-ao-m255* sequences. Each block consisted of a 200 ms linearly frequency modulated (LFM) signals, a 100 ms gap, 0.512 ms pilot signals, the transmitted data and an ending LFM signal. In each block, there were 128 spreading sequences. Thus, the length of each data block was 8.192 s. Information bits were encoded by a rate 1/2 convolutional encoder. Then, the bit rate was 62.5 bit/s. A total of 537 data blocks were transmitted in this experiment.

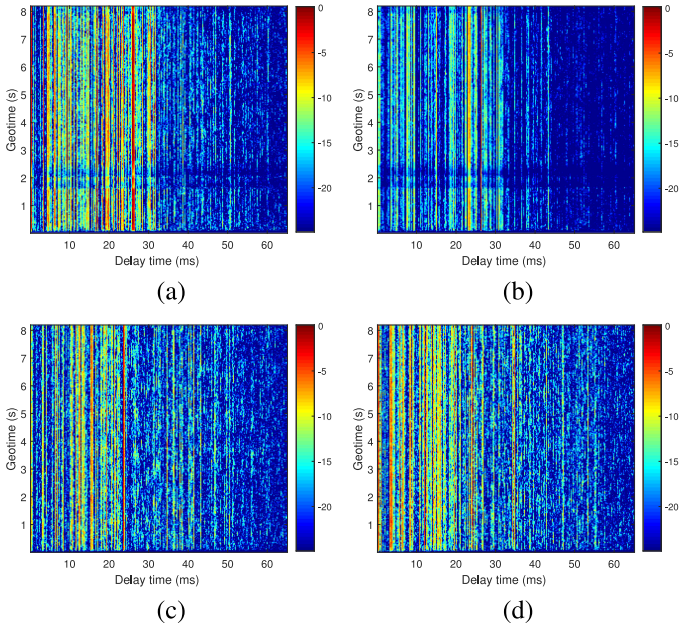

Fig. 10. Examples of CIRs estimated using the IPNLMS algorithm from the DJK data. (a) Estimated channel for the top hydrophone of node 1. (b) Estimated channel for the bottom hydrophone of node 1. (c) Estimated channel for the top hydrophone of node 2. (d) Estimated channel for the bottom hydrophone of node 2.

B. Channel Characteristics

The channels are estimated based on improved proportionate normalized least mean squares (IPNLMS) algorithm. Fig. 10 show the estimated CIR using one transmitted block data for the top and bottle hydrophones of node 1 and node 2. From this figure, we find that the multipath of the channels were very dense. The energy of each tap was relatively average. This channel structures maybe caused by the location of the transducer. The delay spread of the main taps were approximately 30 ms. The corresponding ISI were about 120 chips. The channel structures remained relatively stable over a data block. Meanwhile, as shown in Fig. 10(a) and Fig. 10(b), the channels gain at some point were very small. That maybe caused by impulse noise. Certainly, that will affect the system performance. Compared with node 2, the estimated channels of node 1 were more clear. That was mainly caused by the low received SNR. The measured SNRs were about 5.1 and 3.14 dB for node 1 and node 2, respectively. This makes sense since the transmission distance of node 2 is 400 m farther than that of 1 node.

TABLE I
THE NUMBER OF TRANSMITTED BITS FOR EACH USER UNDER DIFFERENT MULTIUSER SCENARIOS

Number of users	Number of blocks for each user	Total information bits for each user
8	67	34304
10	53	27136
12	44	22528
14	38	19456
16	33	16896

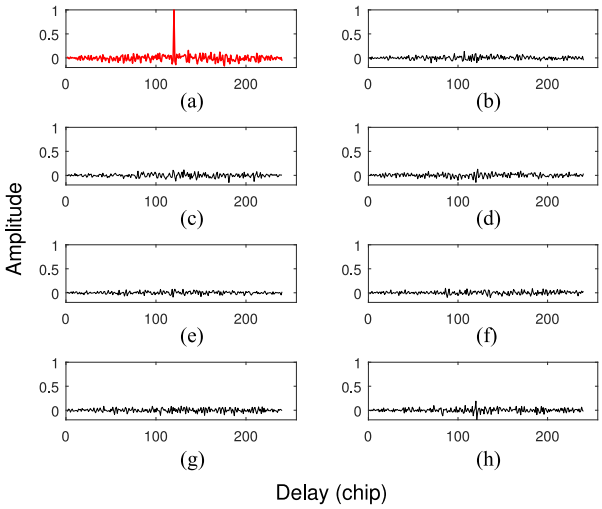

Fig. 11. The equivalent channels for user 1 after PTR processing for 8 users scenarios. (a) Desired channel for user 1. (b) Interference channel from user 2. (c) Interference channel from user 3. (d) Interference channel from user 4. (e) Interference channel from user 5. (f) Interference channel from user 6. (g) Interference channel from user 7. (h) Interference channel from user 8.

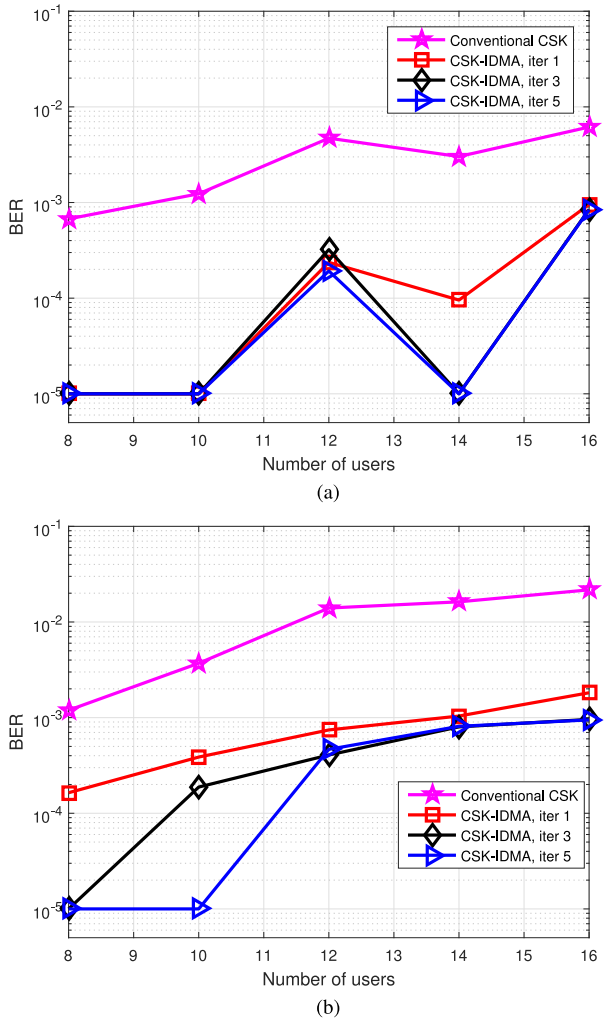

Fig. 12. The BER performance of the proposed method. (a) node 1. (b) node 2.

C. Results

We utilize the received 537 blocks to simulate multiuser scenarios by overlaying the received data. Here we analyze five users scenarios: 8, 10, 12, 14 and 16 users. Table I gives the number of transmitted bits for each user under different multiuser scenarios. We let the transmission interval between each user large enough to make sure the channels of each user are uncorrelated.

We first show the effect of PTR processing. We use the training symbols to reestimate the equivalent channels after PTR processing. Fig. 11 shows the equivalent channels of user 1 after PTR processing for 8 users scenarios with the received data from node 1. The equivalent channels have been normalized. From this figure, we find the desired channel for user 1 is focused and almost could be seen as a single path. Compared with Fig. 10, the desired channel after PTR processing is significantly easier to be equalized. Besides, the power of the desired channel is much larger than that of from other inference users. Thus, the PTR processing offers the spatial-temporal processing gain and improves the SINR.

Fig. 12 gives the BER performance of the proposed method. To further demonstrate the impact of the number of iterations on performance, the numbers of inner-iteration and outer-iteration are 5. We use the received data from all of 8 hydrophones. In this figure, zero BER is denoted by BER $= 10^{-5}$. At node 1, it can realize zero error bits for 8 users, 10 users and 14 users after 5 iterations. The BER is 8.4×10^{-4} for 16 users. At node 2, CSK-IDMA scheme can realize zero error bits for 8 users and 10 users after 5 iterations. The BER for 16 users is 9.7×10^{-4}. Thus, the proposed scheme achieves error-free transmission for 8 and 10 users with data rate of 62.5 bits/s/user within 4 kHz bandwidth. Meanwhile, the performance gap between 3 iterations and 5 iterations are small, which also is shown in the simulation results. From these two subfigures, we find that as the number of users increases, the BER decreases. Meanwhile, the proposed CSK-IDMA scheme is better than conventional CSK scheme. And the gain also degrades with the number of users increases. The performance of CSK-IDMA increases with the number the outer-iteration increases. However, the performance gain of iteration is not obvious.

Fig. 13 gives the BER performance of the proposed method with different hydrophones for 10 users. The number of outer-iteration is 5. Since the performance of PTR improves as the number of hydrophones increases. Thus, more hydrophones are deployed at the receiver, and the BER performance becomes better. The BER is still zero for 10 users with 7 receivers for both

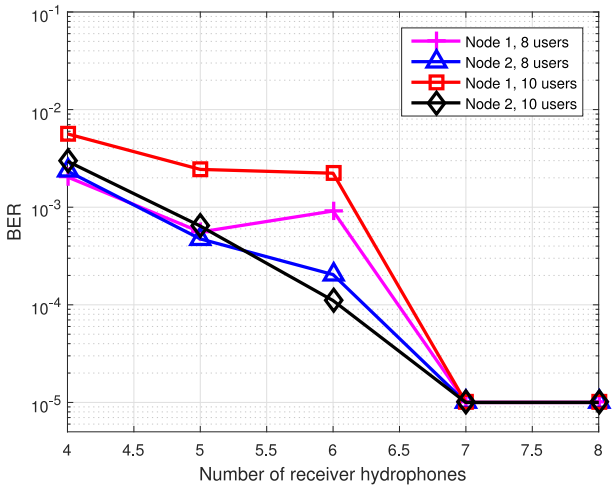

Fig. 13. The BER performance of the proposed method with different hydrophones for 8 users and 10 users.

nodes. An interesting result shown in Fig. 13 is that although the received SNR of node 1 is larger than that of node 2, the BER performance of node 1 with small hydrophones is worse than that of nodes 2. That is because some received blocks are destroyed by the impulse noise in both nodes. That destroyed blocks can not be demodulated entirely. Since the impulse noise did not not destroy all of hydrophones at the same time, its effect is not obvious when the number of hydrophones is large. However, it affects the performance with fewer hydrophones.

VI. Conclusion

In this paper, we proposed a new IDMA scheme for multiuser UWA communications. The proposed scheme adopted CSK modulation to maintain good system data rate. The receiver applied PTR technique to compress the long delay UWA channels and improve the SINR. In order to implement iterative IDMA detection, we proposed a soft decision of CSK demodulation which can iteratively exchanges extrinsic information with a soft channel decoder to achieve turbo system performance. Simulation results demonstrate the superiority of the proposed scheme. We also provide a lake experiment to verify practical feasibility. In this paper, the transmitter and receiver are fixed. Future research will focus on extending the proposed system to mobile asynchronous underwater multiuser communications which need to consider the significant Doppler effect.

References

[1] S. Mahmoudzadeh, D. M. W. Powers, and A. Atyabi, "UUV's hierarchical de-based motion planning in a semi dynamic underwater wireless sensor network," *IEEE Trans. Cybern.*, vol. 49, no. 8, pp. 2992–3005, Aug. 2019.

[2] A. C. Singer, J. K. Nelson, and S. S. Kozat, "Signal processing for underwater acoustic communications," *IEEE Commun. Mag.*, vol. 47, no. 1, pp. 90–96, Jan. 2009.

[3] Y. Zhang, Y. Huang, L. Wan, S. Zhou, X. Shen, and H. Wang, "Adaptive OFDMA with partial CSI for downlink underwater acoustic communications," *J. Commun. Netw.*, vol. 18, no. 3, pp. 387–396, Jun. 2016.

[4] X. Cheng, F. Qu, and L. Yang, "Single carrier FDMA over underwater acoustic channels," in *Proc. 6th Int. ICST Conf. Commun. Netw. China*, Aug. 2011, pp. 1052–1057.

[5] K. Chen, M. Ma, E. Cheng, F. Yuan, and W. Su, "A survey on MAC protocols for underwater wireless sensor networks," *IEEE Commun. Surveys Tuts.*, vol. 16, no. 3, pp. 1433–1447, Jul.–Sep. 2014.

[6] R. Zhang, X. Cheng, X. Cheng, and L. Yang, "Interference-free graph based TDMA protocol for underwater acoustic sensor networks," *IEEE Trans. Veh. Technol.*, vol. 67, no. 5, pp. 4008–4019, May. 2018.

[7] F. Qu, Z. Wang, and L. Yang, "Differential orthogonal space-time block coding modulation for time-variant underwater acoustic channels," *IEEE J. Ocean. Eng.*, vol. 42, no. 1, pp. 188–198, Jan. 2017.

[8] M. Stojanovic and L. Freitag, "Multichannel detection for wideband underwater acoustic CDMA communications," *IEEE J. Ocean. Eng.*, vol. 31, no. 3, pp. 685–695, Jul. 2006.

[9] C. C. Tsimenidis, O. R. Hinton, A. E. Adams, and B. S. Sharif, "Underwater acoustic receiver employing direct-sequence spread spectrum and spatial diversity combining for shallow-water multiaccess networking," *IEEE J. Ocean. Eng.*, vol. 26, no. 4, pp. 594–603, Oct. 2001.

[10] E. Calvo and M. Stojanovic, "Efficient channel-estimation-based multiuser detection for underwater CDMA systems," *IEEE J. Ocean. Eng.*, vol. 33, no. 4, pp. 502–512, Oct. 2008.

[11] S. A. Aliesawi, C. C. Tsimenidis, B. S. Sharif, and M. Johnston, "Iterative multiuser detection for underwater acoustic channels," *IEEE J. Ocean. Eng.*, vol. 36, no. 4, pp. 728–744, Oct. 2011.

[12] T. C. Yang and W. B. Yang, "Interference suppression for code-division multiple-access communications in an underwater acoustic channel," *J. Acoust. Soc. Am.*, vol. 126, no. 1, 2009, Art. no. 220.

[13] T. C. Yang, "Code division multiple access based multiuser underwater acoustic cellular network," *J. Acoust. Soc. Am.*, vol. 130, no. 4, 2011, Art. no. 2347.

[14] G. Yang, Q. Guo, D. Huang, J. Yin, and M. Zheng, "Kalman filter-based chip differential blind adaptive multiuser detection for variably mobile asynchronous underwater multiuser communications," *IEEE Access*, vol. 6, pp. 49 646–49 653, 2018.

[15] G. Yang, J. Yin, D. Huang, L. Jin, and H. Zhou, "A Kalman filter-based blind adaptive multi-user detection algorithm for underwater acoustic networks," *IEEE Sensors J.*, vol. 16, no. 11, pp. 4023–4033, 2016.

[16] T. C. Yang, "Spatially multiplexed CDMA multiuser underwater acoustic communications," *IEEE J. Ocean. Eng.*, vol. 41, no. 1, pp. 217–231, Jan. 2016.

[17] H. C. Song, J. S. Kim, W. S. Hodgkiss, W. A. Kuperman, and M. Stevenson, "High-rate multiuser communications in shallow water," *J. Acoust. Soc. Am.*, vol. 128, no. 5, pp. 2920–2925, 2010.

[18] S. E. Cho, H. C. Song, and W. S. Hodgkiss, "Asynchronous multiuser underwater acoustic communications (l)," *J. Acoust. Soc. Am.*, vol. 132, no. 1, p. 5, 2012.

[19] S. E. Cho, H. C. Song, and W. S. Hodgkiss, "Multiuser acoustic communications with mobile users," *J. Acoust. Soc. Am.*, vol. 133, no. 2, p. 880, 2013.

[20] S. E. Cho, H. C. Song, and W. S. Hodgkiss, "Multiuser interference cancellation in time-varying channels," *J. Acoust. Soc. Am.*, vol. 131, no. 2, pp. 163–9, 2012.

[21] T. C. Yang, "Correlation-based decision-feedback equalizer for underwater acoustic communications," *IEEE J. Ocean. Eng.*, vol. 30, no. 4, pp. 865–880, Oct. 2005.

[22] L. Ping, L. Liu, K. Wu, and W. K. Leung, "Interleave division multiple-access," *IEEE Trans. Wireless Commun.*, vol. 5, no. 4, pp. 938–947, Apr. 2006.

[23] S. Dixit, P. Tripathi, and M. Shukla, "SC-FDMA IDMA scheme for underwater acoustic communications," in *Proc. Commun., Control Intell. Syst.*, 2016, pp. 204–207.

[24] J. Dang, F. Qu, Z. Zhang, and L. Yang, "OFDM-IDMA communications over underwater acoustic channels," in *Proc. Mil. Commun. Conf.*, Nov. 2011, pp. 418–423.

[25] K. Kusume, G. Bauch, and W. Utschick, "IDMA vs. CDMA: Analysis and comparison of two multiple access schemes," *IEEE Trans. Wireless Commun.*, vol. 11, no. 1, pp. 78–87, Jan. 2012.

[26] G. M. Dillard, M. Reuter, J. Zeiddler, and B. Zeidler, "Cyclic code shift keying: A low probability of intercept communication technique," *IEEE Trans. Aerosp. Electron. Syst.*, vol. 39, no. 3, pp. 786–798, Jul. 2003.

[27] C. He, J. Huang, J. Han, and Q. Zhang, "Cyclic shift keying spread spectrum underwater acoustic communication," *Acta Phys. Sin.*, vol. 58, no. 12, pp. 8379–8385, 2009.

[28] C. He, Q. Zhang, and J. Huang, "Passive time reversal communication with cyclic shift keying over underwater acoustic channels," *Appl. Acoust*, vol. 96, pp. 132–138, 2015.
[29] S. Hu, G. Bi, Y. L. Guan, and S. Li, "Spectrally efficient transform domain communication system with quadrature cyclic code shift keying," *IET Commun.*, vol. 7, no. 4, pp. 382–390, 2013.
[30] S. Hu *et al.*, "TDCS-IDMA system for cognitive radio networks with cloud," *IEEE Access*, vol. 6, pp. 20 520–20 530, 2018.
[31] Daniel, O. Julien, M. L. Boucheret, T. Grelier, and L. Ries, "Investigation of CSK as a candidate for future GNSS signals," *Ferroelectrics*, vol. 121, no. 1, pp. 335–342, 2013.
[32] C. He, L. Jing, Q. Zhang, and J. Huang, "Multiuser underwater acoustic communication using cyclic shift keying," in *Proc. OCEANS 2016 - Shanghai*, Apr. 2016, pp. 1–4.
[33] K. H. Kärkkäinen and P. A. Leppänen, "The influence of initial-phases of a PN code set on the performance of an asynchronous DS-CDMA system," *Wireless Pers. Commun.*, vol. 13, no. 3, pp. 279–293, Jun. 2000.

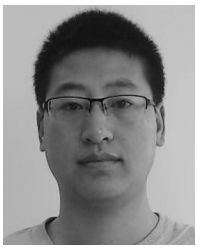

Lianyou Jing received the B.S., M.S., and Ph.D. degrees in the electronic and communications engineering form the School of Marine Science and Technology, Northwestern Polytechnical University, Shaanxi, China, in 2010, 2013, and 2017, respectively. He is currently a Faculty Member with the School of Information and Communication Engineering, Dalian University of Technology. His current research focuses on underwater acoustic communications.

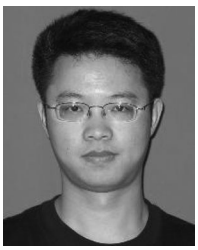

Chengbing He (Member, IEEE) received the B.S., M.S., and Ph.D. degrees in the electronic and communications engineering from the School of Marine Science and Technology, Northwestern Polytechnical University (NPU), Shaanxi, China, in 2003, 2006, and 2009 respectively. He has been a Faculty Member of NPU since then and now is a Professor. His current research focuses on underwater acoustic communications.

Han Wang received the B.S. degree in the electronic and communications engineering from the School of Marine Science and Technology, Northwestern Polytechnical University (NPU), Shaanxi, China, in 2011. She is currently working toward the Ph.D. degree with the School of Marine Science and Technology, NPU. Her current research focuses on under water acoustic communications.

Qunfei Zhang (Member, IEEE) received the B.Sc. degree in electrical engineering and the M.S. degree in signal and information processing from Northwestern Polytechnical University, Xi'an, China, in 1990 and 1993, respectively, and the Ph.D. degree in signal and information processing from Xidian University, Xi'an, China, in 2003. He is currently a Professor with the School of Marine Science and Technology, Northwestern Polytechnical University. His research interests include spectral estimation, array signal processing, underwater communications and networking.

Hongxi Yin received the B.S. degree from Shandong University, Jinan, China, in 1982, the M.E. degree from the Harbin Institute of Technology, Harbin, China, in 1988, and the Ph.D. degree from Zhongshan University, Guangzhou, China, in 1998. From 1998 to 2008, he held a postdoctoral position and an was an Associate Professor with Peking University, China. He was a Research Fellow with the University of Southampton, U.K., from 2005 to 2007. He is currently a Professor with the Dalian University of Technology, Dalian, China. His has coauthored more than 180 journal and conference papers in the areas of optical communication systems and networks. His research interests include advanced optical fiber communication systems and networks, satellite light communication and networking, underwater optical wireless communication and sensor networks, and photonic reservoir computing.